Altered synaptic plasticity and behavioral abnormalities in CNGA3-deficient mice

Michalakis, Stylianos ; Kleppisch, T ; Polta, S A ; Wotjak, Carsten T ; Koch, Susanne ; Rammes, G ; Matt, L ; Becirovic, Elvir ; Biel, Martin

DOI: https://doi.org/10.1111/j.1601-183x.2010.00646.x

Genes, Brain and Behavior
Official publication of the International Behavioural and Neural Genetics Society

Genes, Brain and Behavior (2011) **10:** 137–148 doi: 10.1111/j.1601-183X.2010.00646.x

Altered synaptic plasticity and behavioral abnormalities in CNGA3-deficient mice

S. Michalakis*,†,1, T. Kleppisch‡,1, S. A. Polta§, C. T. Wotjak§, S. Koch†, G. Rammes§,¶, L. Matt‡, E. Becirovic† and M. Biel†

†*Munich Center for Integrated Protein Science CIPS^{M}, Department of Pharmacy – Center for Drug Research, Ludwig-Maximilians-Universität München,* ‡*Institut für Pharmakologie und Toxikologie der Technischen Universität München,* §*Max-Planck-Institut für Psychiatrie, and* ¶*Klinik für Anaesthesiologie der Technischen Universität München, Klinikum rechts der Isar, München, Germany*
**Corresponding author: S. Michalakis, Munich Center for Integrated Protein Science CIPS^{M}, Department of Pharmacy – Center for Drug Research, Ludwig-Maximilians-Universität München, Butenandtstr. 5-13, D-81377 München, Germany.*
E-mail: michalakis@lmu.de

[1] *These authors contributed equally to this work.*

Received 23 December 2009, revised 13 July 2010 and 12 August 2010, accepted for publication 24 August 2010

The role of the cyclic nucleotide-gated (CNG) channel CNGA3 is well established in cone photoreceptors and guanylyl cyclase-D-expressing olfactory neurons. To assess a potential function of CNGA3 in the mouse amygdala and hippocampus, we examined synaptic plasticity and performed a comparative analysis of spatial learning, fear conditioning and step-down avoidance in wild-type mice and CNGA3 null mutants (CNGA3$^{-/-}$). CNGA3$^{-/-}$ mice showed normal basal synaptic transmission in the amygdala and the hippocampus. However, cornu Ammonis (CA1) hippocampal long-term potentiation (LTP) induced by a strong tetanus was significantly enhanced in CNGA3$^{-/-}$ mice as compared with their wild-type littermates. Unlike in the hippocampus, LTP was not significantly altered in the amygdala of CNGA3$^{-/-}$ mice. Enhanced hippocampal LTP did not coincide with changes in hippocampus-dependent learning, as both wild-type and mutant mice showed a similar performance in water maze tasks and contextual fear conditioning, except for a trend toward higher step-down latencies in a passive avoidance task. In contrast, CNGA3$^{-/-}$ mice showed markedly reduced freezing to the conditioned tone in the amygdala-dependent cued fear conditioning task. In conclusion, our study adds a new entry on the list of physiological functions of the CNGA3 channel. Despite the dissociation between physiological and behavioral parameters, our data describe a so far unrecognized role of CNGA3 in modulation of hippocampal plasticity and amydgala-dependent fear memory.

Keywords: Amygdala, cyclic nucleotide-gated channel, fear conditioning, hippocampus, long-term potentiation, spatial learning

Cyclic nucleotide-gated (CNG) channels open in response to binding of cyclic adenosine monophosphate (cAMP) and cyclic guanosine monophosphate (cGMP). When activated, these channels pass a mixed Na^+/Ca^{2+} inward current causing depolarization of the plasma membrane and an increase in the cytosolic Ca^{2+} concentration (Biel & Michalakis 2009; Craven & Zagotta 2006; Kaupp & Seifert 2002). Cyclic nucleotide-gated channels play a key role in the signal transduction pathways of photoreceptors and olfactory sensory neurons (Biel & Michalakis 2007; Craven & Zagotta 2006; Kaupp & Seifert 2002). In contrast, it is not clear whether or not these channels have functions in other types of neurons. So far, only a few reports postulated a role of CNG channels in the brain. The olfactory CNG channel (CNGA2) was hypothesized to modulate neurotransmission between olfactory nerve fibers and their target neurons in the olfactory bulb (Murphy & Isaacson 2003). In addition, a study in hippocampal pyramidal neurons suggested that CNG channels contribute to the generation of plateau potentials induced by muscarinic receptor activation (Kuzmiski & MacVicar 2001). Finally, analysis of mice lacking the CNGA2 subunit showed an impairment of long-term potentiation (LTP) in the Schaffer collateral pathway, indicating that this channel may support the induction of hippocampal CA1 LTP (Parent *et al*. 1998). To date, no report exists on potential central nervous system (CNS) functions of the cone photoreceptor type channel CNGA3. Loss of CNGA3 function is known to result in total color blindness in humans (Kohl *et al*. 1998) and mice (Biel *et al*. 1999). CNGA3 is also important for the generation of sensory responses in guanylyl cyclase-D (GC-D) type non-canonical olfactory neurons (Leinders-Zufall *et al*. 2007; Munger *et al*. 2009). The goal of the present study was to identify potential functions of CNGA3 in the amygdala and hippocampus by examining its expression, synaptic plasticity and related behavioral paradigms in wild-type (WT) mice and CNGA3 null mutants (CNGA3$^{-/-}$).

Materials and methods

Animals

The generation of CNGA3$^{-/-}$ mice has been described previously (Biel *et al*. 1999). Mice with pure genetic background were obtained by backcrossing the original CNGA3$^{-/-}$ mice of mixed C57BL/6N × 129Sv genetic background for 10 or more generations to C57BL/6N (Charles River, Sulzfeld, Germany) or 129Sv (129S2/SvHsd; Harlan Winkelmann, Borchen, Germany) background, respectively. If not

stated otherwise, CNGA3 mutants and litter-matched control mice ($CNGA3^{+/+}$) of C57BL/6N genetic background were used for experiments. Test animals were derived from heterozygous breeding pairs, which yielded equivalent numbers of mutant and WT mice. All experiments conform to the German animal protection laws. Behavioral procedures were approved by the Committee on Animal Health and Care.

Semiquantitative RT-PCR

Hippocampi were dissected from freshly isolated brains. Basolateral amygdala complexes (BLACs) were isolated from shock-frozen brains as described previously (Marsicano *et al*. 2002). Subsequently, mRNA was isolated using oligo (dT)-DynaBeads (Invitrogen, Karlsruhe, Germany). Oligo-dT-primed first-strand cDNA was synthesized with Superscript II H^- reverse transcriptase (Invitrogen). Equal amounts of cDNA (representing about 16 mg of hippocampus or 800 μg of amygdala tissue) were used to amplify (30 cycles for hippocampus, 35 cycles for BLAC) CNG-specific transcripts. The housekeeping gene hypoxanthine phosphoribosyltransferase (HPRT) served as an internal standard and was amplified by 22 cycles. Equal amounts of individual polymerase chain reactions (PCRs) were separated on 5% polyacrylamide gels. Amplicons were stained with ethidium bromide and analyzed densitometrically on a Gel Doc 2000 System using the Quantity One software v 4.2.3 (Biorad, Munich, Germany). For every reaction, the intensity of a CNG channel amplicon was normalized to the intensity of the HPRT amplicon obtained from the same cDNA. The specificity of the amplicons was verified by restriction analysis and sequencing. The primer sequences are available on request.

Western blot

Amygdala and hippocampal tissues were dissected from vibratome sections and snap-frozen in liquid nitrogen. Brain and retinal tissue samples were homogenized on dry ice using a mortar and pestle, boiled in lysis buffer [2% sodium dodecyl sulphate (SDS), 50 mM Tris] for 10 min and centrifuged (15 min at 16 000 ***g***) to remove cell debris. Equal amounts of protein were separated using 7% sodium dodecyl sulphate–polyacrylamide gel electrophoresis (SDS–PAGE) followed by Western blot analysis according to standard procedures. The affinity-purified anti-CNGA3 antibody (Biel *et al*. 1999) was used at 1:3000 dilution.

Immunohistochemistry

Twelve-μm-thick coronal cryosections of shock-frozen mouse brains were fixed in 1% paraformaldehyde for 10 min. The sections were incubated for 16 h at 4°C with phosphate-buffered saline (PBS) containing affinity-purified anti-CNGA3 antibody (Biel *et al*. 1999) at 1:3000 dilution, 5% Chemiblocker (CB, Millipore, Schwalbach, Germany) and 0.3% Triton-X-100. Endogenous peroxidase activity was quenched using 3% H_2O_2 in methanol. Secondary detection was performed for 1 h with horseradish peroxidase-labeled donkey anti-rabbit antibody (Jackson Immunoresearch, Newmarket, UK) in PBS/2% CB followed by tyramide signal amplification (TSA) plus Cy3 system (Cy3-TSA 1:200, 7 min; Perkin Elmer, Rodgau, Germany). Cell nuclei were stained with Hoechst 33342 (Invitrogen). The slides were coverslipped with Fluoromount-G mounting medium (Beckmann-Coulter, Krefeld, Germany) and examined on a Zeiss confocal laser scanning microscope (LSM 510 Meta, Zeiss, Oberkochen, Germany).

Behavioral analysis

Mice were housed singly for at least 2 weeks before starting the experiments and kept under an inverse 12-h light/dark cycle (lights off at 0800 h).

Fear conditioning

Three- to 6-month-old $CNGA3^{-/-}$ male mice and litter-matched controls were transferred from their home cages into conditioning chambers (illumination: 0.6 lux) with shock floors (MED Associates, St Albans, VT, USA). Three minutes later, a 20-second tone (9 kHz, sine waves, 80 dB) was presented that coterminated with an electric footshock (2 seconds, 0.7 mA). Mice were returned to their home cages 1 min after the tone ended. The next day, mice were re-exposed to the conditioning context for 3 min without tone presentation. Four hours after testing contextual fear, mice were placed into a neutral context (Plexiglass cylinder differing from the conditioning chamber in shape, material, bedding and odor of the cleaning solution; Kamprath & Wotjak 2004; illumination: 0.3 lux), and a 180-second tone (9 kHz, sine waves, 80 dB) was presented after a control period of 3 min. Freezing was defined and scored essentially as described before (Kamprath & Wotjak 2004). Freezing behavior was defined as the absence of all movements, except for respiration, and served as a correlate of conditioned fear. All sessions were videotaped and analyzed off-line by means of customized software. We assessed the duration of freezing episodes displayed in the conditioning chamber and the neutral environment before tone presentation (intensity and specificity of *contextual fear memory*) and during tone presentation (*cued memory*) 24 h after conditioning. Data were normalized to the total length of the respective observation period.

Sensitization

To assess the role of sensitization (i.e. non-associative changes in fear responsiveness; Kamprath & Wotjak 2004), another batch of animals was placed into the conditioning chamber and received an unsignaled footshock (0.7 mA, 2 seconds) after 198 seconds. Mice were returned to their home cages after additional 60 seconds. Foreground contextual fear was assessed by placing the animals back to the conditioning context for 3 min 24 h later, followed by measurement of sensitized fear by exposure to a 3-min tone in the test context another 4 h later (see above).

Acoustic startle responses

Naïve mice were placed into one out of seven identical startle setups, consisting of a non-restrictive Plexiglass cylinder (inner diameter 4 cm, length 8 cm) mounted onto a plastic platform, each housed in a sound-attenuated chamber (SR-LAB, San Diego Instruments SDI, San Diego, CA, USA). The cylinder movement was detected by a piezoelectric element mounted under each platform and the voltage output of the piezo was amplified and then digitized (sampling rate: 1 kHz) by a computer interface (I/O-board provided by SDI). The startle amplitude was defined as the peak voltage output within the first 50 milliseconds after stimulus onset and quantified by means of SR-LAB software. Before startle measurements, we calibrated response sensitivities for each chamber to assure identical output levels. Startle stimuli and background noise were delivered through a high-frequency speaker placed 20 cm above each cage. The startle stimuli consisted of white noise bursts of 20-millisecond duration and 75, 90, 105 or 115 dB(A) intensity (INT) presented in a constant background noise of 50 dB(A). Intensity was measured using an audiometer (Radio Shack, 33-2055; RadioShack, Fort Worth, TX, USA). On control trials, only background noise was present. After an acclimation period of 5-min duration, 10 control trials and 20 startle stimuli of each intensity were presented in pseudorandom order in each test session. The interstimulus interval was 15 seconds averaged (13–17 seconds, pseudorandomized). Plexiglass cylinders were cleaned thoroughly with soap water after each trial. Experiments were performed in the dark (0 lux) with red light in the experimental room. Acoustic startle responses (ASRs) to a given stimulus intensity were averaged separately for each mouse.

Prepulse facilitation/inhibition

Mice were again tested in the startle apparatus 24 h after completion of the ASR measurements. This time, ASRs were elicited using stimuli (ASRS) of 115 dB(A) intensity with a duration of 20 milliseconds at a background noise level of 50 dB(A). Each test session consisted of a 5-min acclimation period followed by 20 ASRS for habituation to the ASR-eliciting stimulus. Another 22 ASRS, 210 prepulse (PP) condition trials and 18 PP control trials were arranged

in a pseudorandomised order, where no stimulus condition was presented repeatedly more than once. Intertrial interval (ITI) was 15 seconds averaged, ranging from 13 to 17 seconds; 15 different PP conditions were presented, each for 14 times. Three different PP intensities were used [55, 65 or 75 dB(A)] with an interpulse interval (IPI, prepulse onset to stimulus onset) of 5, 10, 25, 50 or 100 milliseconds. The PP duration was 10 milliseconds unless the IPI was 5 milliseconds.

On PP control trials only the PP was presented. Each of the three intensities was presented six times. Prepulse inhibition (PPI) and prepulse facilitation (PPF) of each mouse (i) were expressed as percent change of the ASR (ΔASR) calculated as follows:

$$\Delta\mathrm{ASR}_i = \left(\frac{\mathrm{PS}_i - \mathrm{S}_i}{\mathrm{S}_i}\right) \cdot 100\%$$

where PS_i is the averaged response preceded by a PP and S_i the averaged response without PP for each mouse, respectively. Responses per IPI and PP intensity were averaged for each mouse.

Discriminatory water maze

Four weeks after fear conditioning, mice were habituated to the water and tested in a discriminatory water maze task (Arns *et al*. 1999; Moosmang *et al*. 2005). In this task, animals had to learn to discriminate between two visible platforms (10 cm in diameter) that were placed in a circular swimming pool (80 cm in diameter, 30 cm high, white plastic) filled with water (22 ± 1°C, made opaque-white using non-toxic water dye) up to a depth of 20 cm. One platform was stable and kept in a fixed position (correct choice); the other platform changed position from trial to trial in a pseudorandom order and sank when a mouse climbed onto it (incorrect choice). The test was conducted at 1.0 ± 0.1 lux in order to ensure that the vision is totally conferred by the rod photoreceptor system, which is not impaired in CNGA3$^{-/-}$ mice (Biel *et al*. 1999). Distal spatial cues were provided by the lab environment and sparely illuminated. Trials were terminated either if the mouse climbed onto one of the two platforms or if 30 seconds had elapsed. In case of wrong decisions or omissions, mice were placed on the 'correct' platform, where all animals remained for 10 seconds before they were returned to their home cages. Platforms were cleaned thoroughly between all trials to remove potential proximal cues (e.g. urine). Learning was assessed during initial five training sessions (days 1–5). Each session included 10 trials separated by 2–4-min intermissions. From day 6 on, the fixed platform was moved to a different place, and mice were trained for the new platform position in another four training sessions (days 6–9; relearning). The number of correct choices (expressed as the percentage of the total number of choices per session) and the escape latencies were used to assess memory performance.

Morris water maze

Different batches of mice were habituated to the water the day before the experiment. On days 1–3, animals had to learn to locate a stable platform (10 cm in diameter, 0.5 cm below the water level) that was placed in a circular swimming pool (120 cm in diameter, 70 cm high, white plastic) filled with water (22 ± 1°C, made opaque-white using non-toxic water dye) up to a depth of 30 cm. The test was conducted at 0.4 ± 0.1 lux in order to ensure that the vision is totally conferred by the rod photoreceptor system. An infrared illumination box (TSE, Bad Homburg, Germany) was placed under the water maze. The VideoMot2 system (TSE) equipped with an infrared camera was used for data acquisition and analysis. Distal spatial cues (a black circle, a rectangle and a triangle) were positioned at the maze walls. Trials were terminated either if the mouse climbed onto the platform or if 120 seconds had elapsed. In case of omissions, mice were placed on the platform, where all animals remained for 10 seconds before they were returned to their home cages. The platform was cleaned thoroughly between all trials to remove potential proximal cues (e.g. urine). Spatial learning was assessed during initial three training sessions (days 1–3). The escape latencies were used to assess memory performance. Each session included six trials separated by 15-min intermissions. On day 4, the fixed platform was removed and reference memory was assessed in a single probe trial (1 min).

Forced swim test

Mice were placed into glass cylinders (height: 25 cm, diameter: 17.5 cm) that were filled with 25°C (±1°C) warm water to a height of 12 cm. The behavior of the animals was videotaped over the course of the 6-min exposure. This procedure was repeated the next day. The time the mice spent floating was analyzed off-line and normalized for the respective observation period.

Step-down avoidance learning

Three weeks after the Morris water maze, mice were placed onto a platform (2.5 × 10 × 10 cm^3) and received a scrambled electric foot shock (0.7 mA) when they stepped off the platform onto a metal grid. Mice were returned to their home cages immediately after the foot shock. Passive avoidance memory was tested by placing the mice back onto the platform 24 h later and measuring step-down latencies (four paws criterion) in three consecutive trials. Trials were terminated after 5 min in cases of failure to step down; a step-down latency of 301 seconds was ascribed to the trial. The mean of the three trials served as a measure of memory performance (Murgatroyd *et al*. 2009).

Field potential recordings in the CA1 region of the hippocampus and the amygdala

Field excitatory postsynaptic potentials (fEPSPs) in the CA1 region of transverse hippocampal slices (400 μm thick) from CNGA3$^{+/+}$ and CNGA3$^{-/-}$ mice (3–4 months of age) were recorded as described (Kleppisch *et al*. 1999). Briefly, Schaffer collaterals of hippocampal slices kept in a submersion type recording chamber perfused (1–2 ml/min) with artificial cerebrospinal fluid (ACSF) (Kleppisch *et al*. 1999) were stimulated by square pulses (0.066 Hz, 100 μs) delivered via a monopolar tungsten electrode. Postsynaptic signals were recorded using glass pipettes filled with NaCl (3 mM) located in the CA1 region and an AXOCLAMP 2B amplifier (Axon Instruments, Foster City, CA, USA). PULSE software (HEKA, Lambrecht, Germany) was utilized to control stimulation and data acquisition via an ITC-16 computer interface (HEKA). To induce LTP in the CA1 region, a weak tetanus (50 Hz lasting 1 second) and a strong tetanus (3 × 30 pulses at 100 Hz with a pause of 5 seconds) were applied with 1-h intermission. Long-term depression (LTD) was induced using a paired-pulse stimulation (900 pulse pairs at 1 Hz, 50-millisecond interstimulus interval) adapted from Kemp and Bashir (1997). The fEPSP slope was used to assess the strength of synaptic transmission. For all recordings, the stimulus intensity was adjusted to elicit approximately 40–50% of the maximal fEPSP amplitude. The same intensity was used during tetanus. Long-term potentiation and LTD were expressed as percentage of the fEPSP during the baseline recording.

Field potentials (FPs) in the lateral and basolateral amygdala (LA and BLA, respectively) were evoked by square pulse stimuli (0.066 Hz, 10–20 V, 50 μs) delivered via bipolar tungsten electrodes. The stimulation electrodes were positioned on the border between the LA and the external capsule. Field potentials were recorded using glass microelectrodes (1–2 MΩ) filled with ACSF as described previously (Rammes *et al*. 2000) in the LA or the BLA. The stimulus intensities were adjusted to produce an FP of about 50% of the maximum amplitude. Low frequency stimulation (LFS, 900 pulses at 1 Hz) and high frequency stimulation (HFS, 2 × 50 Hz/1 second, 10-second interstimulus interval) were applied to induce LTD and LTP, respectively, at the same stimulus intensity. The amplitude of FPs was calculated as $(a + b)/2$, where (a) is the voltage difference between the sharp negative onset and the negative peak and (b) is the voltage difference between the negative peak and the succeeding positive peak. Four consecutive FPs were averaged into one response. Therefore, each dot in the graph represents the normalized amplitude of one averaged trace and is equal to 1 min.

Statistics

All data are presented as mean ± standard error of the mean (SEM). Data were analyzed by paired and unpaired t-test or analysis of variances (ANOVAs) as indicated in the text. *Post hoc*

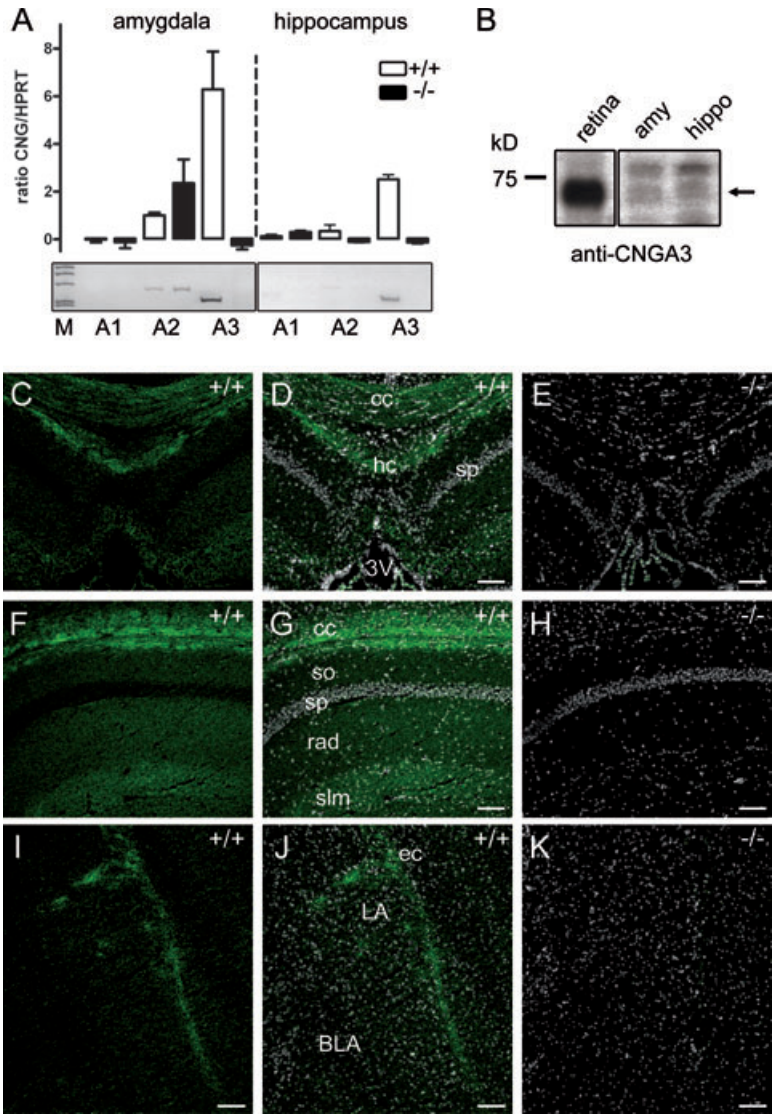

Figure 1: Expression of CNGA3 in mouse amygdala and hippocampus. (A) Semiquantitative RT-PCR analysis of expression levels of CNG channel subunits (A1–A3) in the amygdala and hippocampus of CNGA3$^{+/+}$ (white bars, $n = 3$) and CNGA3$^{-/-}$ mice (black bars, $n = 3$). The *HPRT* gene was used as an internal standard to normalize data obtained from individual amplification reactions (see *Materials and Methods*). (A) Western blot of homogenates from mouse retina, amygdala (amy) and hippocampus (hippo) probed with anti-CNGA3. The arrow indicates the expected size of 70 kD. (C–K) Immunolocalization of the CNGA3 protein (green) in the hippocampus (C–H) and the amygdala (I–K) of wild-type (C, D, F, G,I and J) or CNGA3$^{-/-}$ (E, H AND K) mice. Cell nuclei were stained with Hoechst 33342 (gray) in D, E, G, H, J and K. Scale bar is 100 μm. 3V, third ventricle; cc, corpus callosum; ec, external capsule; hc, hippocampal commissure; rad, stratum radiatum; slm, stratum lacunosum moleculare; so, stratum oriens; sp, stratum pyramidale.

analyses were performed by Newman–Keuls test, if appropriate. Long-term potentiation data were log-transformed before analysis to ensure normal distribution of the data. Statistical significance was accepted if $P \leq 0.05$. All electrophysiological and behavioral experiments were performed and analyzed blindly to the animals' genotype.

Results

Expression of CNGA3 in mouse amygdala and hippocampus

All native CNG channels contain one type of principal A subunit (CNGA1–3) and corresponding modulatory subunits (CNGA4 and/or CNGB1 and B3). We analyzed the relative expression levels of the three A subunits in the amygdala and the hippocampus of WT and CNGA3$^{-/-}$ mice using a semiquantitative reverse transcriptase-PCR (RT-PCR) approach. The CNGA3 subunit was the most abundantly expressed A subunit in both brain regions analyzed. As expected, no signal was detected in the knockout (KO) samples (Fig. 1A). Deletion of CNGA3 did neither significantly alter the expression levels of other CNG channel subunits nor affect the gross brain anatomy (not shown). In addition, we studied the expression of CNGA3 using an anti-CNGA3 antibody that was previously shown to specifically detect CNGA3 in the mouse retina (Biel *et al*. 1999; Michalakis *et al*. 2005). Western blot analysis identified very low amounts of CNGA3 protein in amygdala and hippocampus of WT mice (Fig. 1B). We further characterized the localization of CNGA3 protein by immunohistochemistry (Fig. 1C–K). Using tyramide signal amplification, we found weak CNGA3-specific labeling in sections from WT mice (Fig. 1C,D,F,G,I,J) that was absent in CNGA3$^{-/-}$ mice (Fig. 1E,H,K). The labeling was found in neuronal fibers of the external and internal capsules (Fig. 1C), the hippocampal commissure and the corpus callosum (Fig. 1D,G,J). In addition, we observed very

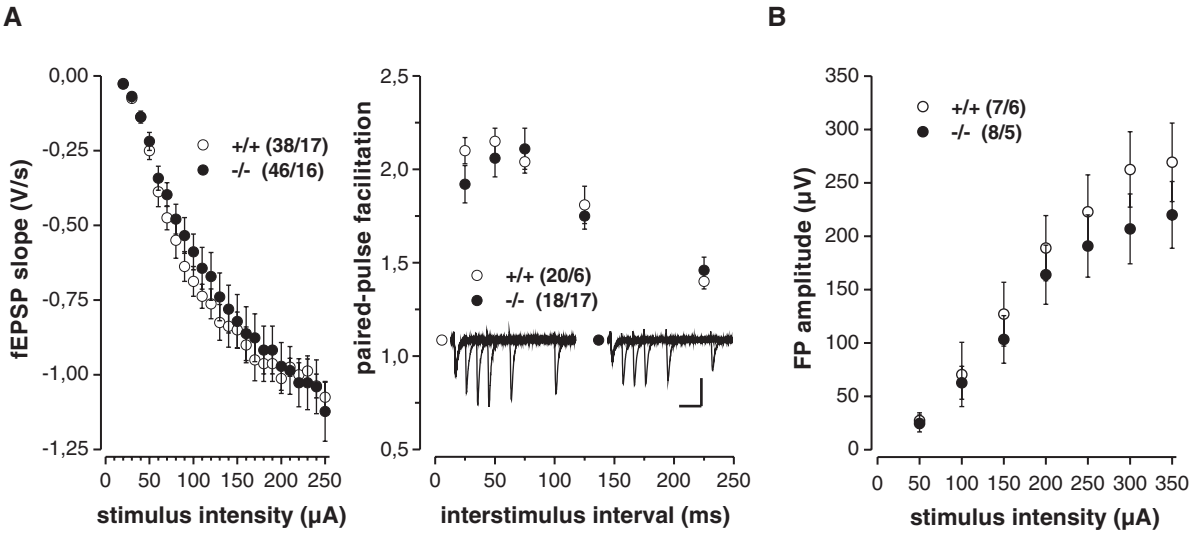

Figure 2: CNGA3$^{-/-}$ mice show normal basal synaptic transmission. Hippocampal or amygdala slices were prepared from adult CNGA3$^{+/+}$ (○) and CNGA3$^{-/-}$ (●) mice. (A) Input–output relation (left) and paired-pulse facilitation (right) of CNGA3$^{+/+}$ and CNGA3$^{-/-}$ mice. Field excitatory postsynaptic potentials were recorded in the CA1 region of the hippocampus after stimulation of the Schaffer collaterals. Representative fEPSPs elicited by pulse pairs with interstimulus intervals of 25, 50, 75, 125 and 225 milliseconds are superimposed in the corresponding insets. Scale: 50 milliseconds, 0.5 mV. (B) Input–output relation of CNGA3$^{+/+}$ and CNGA3$^{-/-}$ mice. Field potentials were recorded in the lateral amygdala after stimulation of the external capsule. Sample size is given in brackets with the first number indicating the number of slices and the second the number of animals analyzed.

weak labeling in the stratum oriens, stratum moleculare and stratum lacunosum moleculare of the hippocampus, as well as within the LA and BLA.

Mice lacking CNGA3 exhibit normal basic characteristics of synaptic transmission

Given the presence of CNGA3 in mouse hippocampus and amygdala, we wondered whether or not this ion channel is a regulator of synaptic transmission in these brain regions. To test for a potential universal defect of synaptic transmission because of the deletion of the *CNGA3* gene, we evaluated the dependency of the fEPSP slope in the CA1 region of the hippocampus or the FP amplitude in the BLA on the stimulus intensity (input–output relation, IOR) of WT and CNGA3$^{-/-}$ mice. In the CA1 region of the hippocampus, we also measured paired-pulse facilitation. As none of these parameters were notably different between the two genotypes (Fig. 2), we conclude that basal synaptic transmission was not altered in the hippocampus and the amygdala of CNGA3$^{-/-}$ mice.

Deletion of the CNGA3 gene results in specific enhancement of LTP in the CA1 region

To evaluate the role of CNGA3 in synaptic plasticity, we next examined LTP in the CA1 region in response to a weak (50 Hz) and a strong (100 Hz) tetanus applied consecutively with 1-h pause. Initially, we used litter-matched WT and CNGA3$^{-/-}$ mice derived from a C57BL/6N genetic background. Sixty minutes following the weak tetanus, the fEPSP slope amounted to 123.6 ± 6.5% (WT) and 141.0 ± 7.3% (CNGA3$^{-/-}$). To analyze the data by two-way ANOVA (*genotype*, *time*) for repeated measures (*time*), we averaged and log-transformed every five consecutive data points after LTP induction. Analysis showed a significant main effect of *genotype* ($F_{1,29} = 5.9$, $P = 0.021$), but no significant factorial interactions (Fig. 3A). After the additional strong tetanus, the difference in LTP between CNGA3$^{-/-}$ mice (176.6 ± 11.7%) and their WT littermate controls (145.8 ± 7.6%) further increased significantly (*genotype*: $F_{1,29} = 4.5$, $P = 0.042$; Fig. 3A). To substantiate these findings and to exclude a possible effect of the genetic background, we repeated these experiments using WT and CNGA3$^{-/-}$ mice with a pure 129Sv background (Fig. 3B). Long-term potentiation was not statistically significantly different between the two genotypes following the first 50-Hz tetanus (WT: 117.3 ± 3.6%; CNGA3$^{-/-}$: 122.1 ± 4.7%; *genotype*: $F_{1,21} = 0.2$, $P = 0.670$). However, following the subsequent 100-Hz tetanus, LTP in CNGA3$^{-/-}$ mice was higher than in the WT controls (155.2 ± 5.5% and 133.6 ± 8.0%, respectively; *genotype*: $F_{1,21} = 4.2$, $P = 0.05$; Fig. 3B).

We next examined LTP in the LA (Fig. 3C) and BLA (Fig. 3D) of WT and CNGA3$^{-/-}$ littermates. A strong tetanus (5 × 100 Hz/1 second, 10-second interstimulus interval) induced LTP in both regions and genotypes. However, unlike in the hippocampus, LTP in the amygdala was not statistically different between control and mutant mice in the LA (*genotype*: $F_{1,25} = 2.05$, $P = 0.164$; *genotype* × *interval:* $F_{11,275} = 0.855$, $P = 0.586$; Fig. 3C) and BLA (*genotype*: $F_{1,22} = 1.628$, $P = 0.215$; *genotype* × *interval:* $F_{9,198} = 0.629$, $P = 0.771$; Fig. 3D). Long-term depression was similar for CNGA3$^{-/-}$ and CNGA3$^{+/+}$ mice both

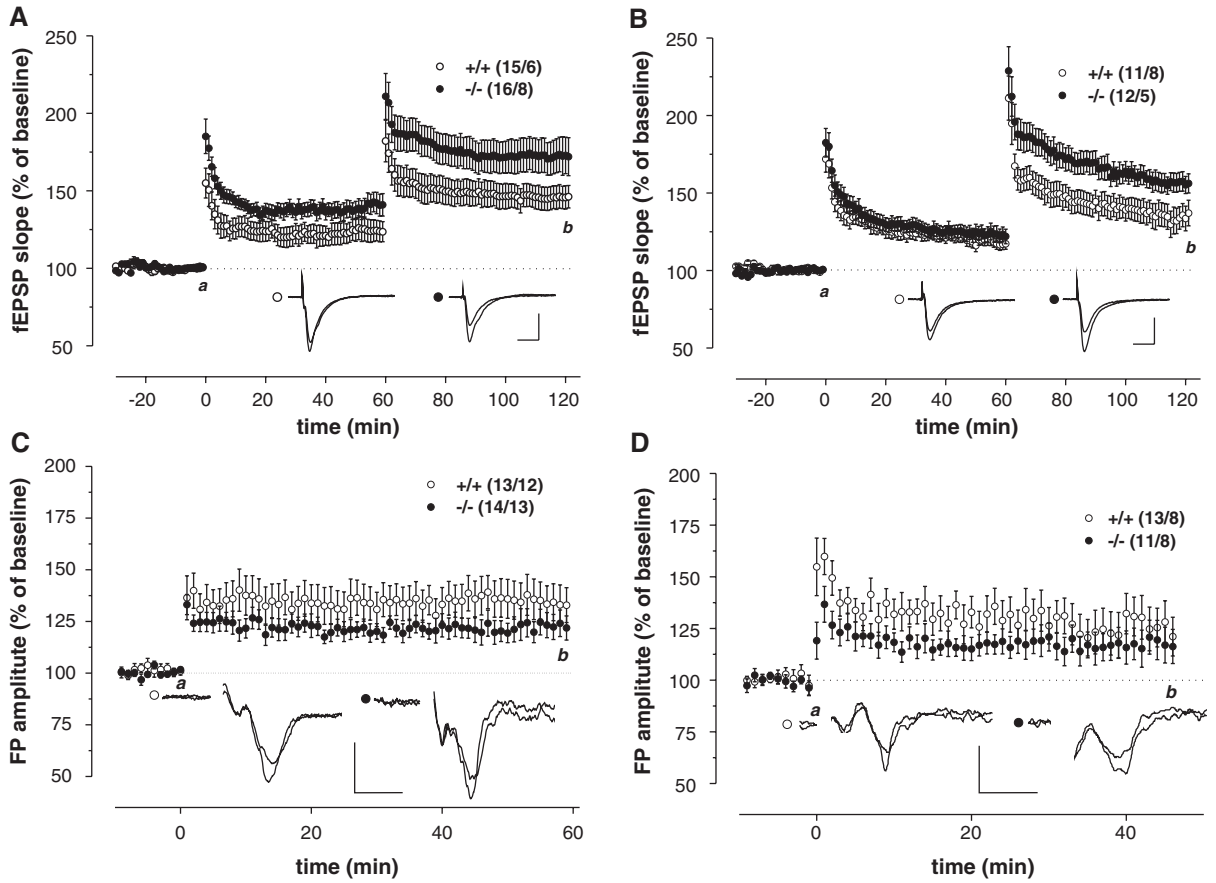

Figure 3: CNGA3$^{-/-}$ mice show increased LTP in the hippocampus, but normal LTP in the amygdala. Hippocampal or amygdala slices were prepared from adult CNGA3$^{+/+}$ (○) and CNGA3$^{-/-}$ (●) mice. Sample size is given in brackets with the first number indicating the number of slices and the second the number of animals analyzed. (A and B) Hippocampal LTP in slices from litter-matched CNGA3$^{+/+}$ and CNGA3$^{-/-}$ mice with a C57BL/6N (A) or 129Sv (B) genetic background. Field excitatory postsynaptic potentials were recorded in the CA1 region of the hippocampus after stimulation of the Schaffer collaterals. Long-term potentiation was induced by a 50-Hz tetanus (at time 0 min). An additional 100-Hz tetanus was applied 60 min after the 50-Hz tetanus. (C and D) Amygdala LTP in slices from litter-matched CNGA3$^{+/+}$ and CNGA3$^{-/-}$ mice with a C57BL/6N genetic background. Field potentials were recorded (C) in the lateral amygdala after stimulation of the external capsule or (D) in the basolateral amygdala after stimulation of the lateral amygdala. Long-term potentiation was induced by a 50-Hz tetanus (at time 0 min). Data represent the mean ± SEM. Representative fEPSPs or FPs recorded at times indicated (*a* and *b*) are illustrated in the corresponding inset. Scale bars in (A) and (B): 10 milliseconds, 0.5 mV; in (C) and (D): 5 milliseconds, 0.2 mV.

within hippocampus (*genotype*: $F_{1,16} = 0.055$, $P = 0.818$; *genotype* × *interval*: $F_{8,128} = 0.838$, $P = 0.571$; Fig. 4A) and amygdala (*genotype*: $F_{1,8} = 0.343$, $P = 0.574$; *genotype* × *interval*: $F_{8,64} = 0.203$, $P = 0.989$; Fig. 4B). Consequently, the deletion of the *CNGA3* gene results in a hippocampus-specific increase in LTP following a strong tetanus.

Normal spatial learning in CNGA3$^{-/-}$ mice

We next tested whether the enhancement of LTP in CNGA3 KO mice has any effects on hippocampus-dependent spatial learning. To countervail the functional impairment of daylight vision in CNGA3$^{-/-}$ mice (Biel *et al*. 1999), we designed a spatial learning test under low light conditions (see *Materials and methods*). In the two platform discriminatory water maze test (2P water maze), experimental animals showed a decrease in escape latencies over the course of the five training sessions (factor *time*: $F_{8,176} = 57.9$, $P < 0.0001$), reaching an asymptotic level during the reversal trials (Fig. 5A). There was a significant difference between the two genotypes ($F_{1,22} = 8.1$, $P = 0.009$) but no significant *genotype* × *time* interaction, indicating that CNGA3$^{-/-}$ took somewhat longer to reach one of the two platforms, compared with WT controls. The slightly longer latency times of CNGA3$^{-/-}$ mice observed at days 3 and 4 cannot be explained by the differences in stress coping behavior, as both genotypes showed a similar behavioral performance in the forced swim test [2-way ANOVA (genotype, day) for repeated measures: *genotype*: $F_{1,18} = 0.324$, $P = 0.576$; *day*: $F_{1,18} = 46.2$, $P < 0.001$; *genotype* × *day*: $F_{1,18} = 0.106$, $P = 0.748$; Fig. 5C].

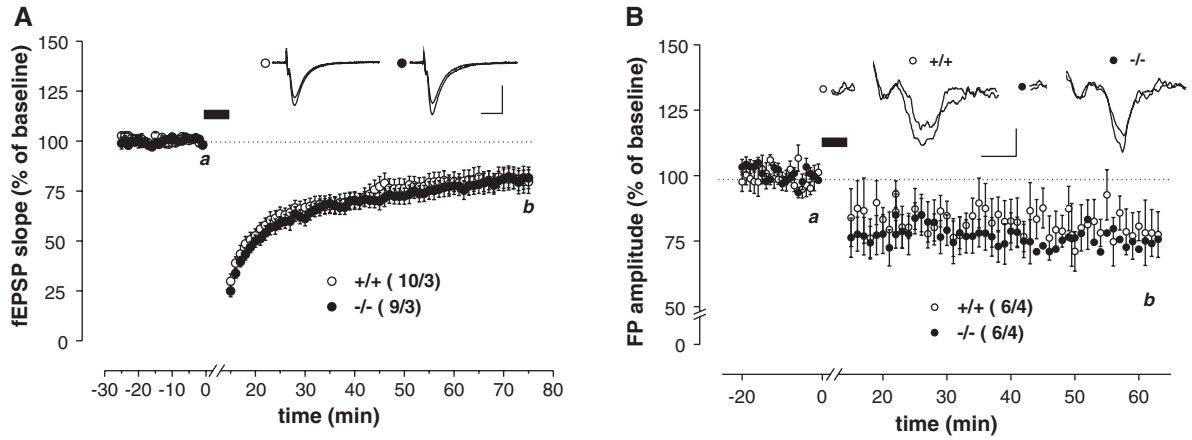

Figure 4: CNGA3$^{-/-}$ mice show normal hippocampal and amygdala LTD. Hippocampal or amygdala slices were prepared from adult CNGA3$^{+/+}$ (○) and CNGA3$^{-/-}$ (●) mice. (A) Hippocampal LTD in slices from litter-matched CNGA3$^{+/+}$ and CNGA3$^{-/-}$ mice with a 129Sv genetic background. Field excitatory postsynaptic potentials were recorded in the CA1 region of the hippocampus after stimulation of the Schaffer collaterals. Long-term depression was induced by a 1-Hz paired-pulse protocol (900 pulse pairs) starting at time 0. (B) Amygdala LTD in slices from litter-matched CNGA3$^{+/+}$ and CNGA3$^{-/-}$ mice with a C57BL/6N genetic background. Field potentials were recorded in the basolateral amygdala after stimulation of the lateral amygdala. Long-term depression was induced by a 1-Hz paired-pulse protocol (900 pulse pairs) starting at time 0. Data represent the mean ± SEM. Representative fEPSPs recorded at times indicated (*a* and *b*) are illustrated in the corresponding inset. Scale bars in (A) and (B): 10 milliseconds, 0.5 mV.

With respect to spatial learning in the 2P water maze, both CNGA3$^{+/+}$ and CNGA3$^{-/-}$ mice developed a clear preference for the fixed platform position over the course of the five training trials as indicated by the high number of correct choices (*day*: $F_{4,88} = 20.1$, $P < 0.0001$; Fig. 5B) with no differences between the genotypes (*genotype*: $F_{1,22} = 0.331$, $P = 0.571$; *genotype* × *day*: $F_{4,88} = 0.130$, $P = 0.971$). After platform reversal, there was a significant decrease in the number of correct choices compared to day 5 in either genotype ($P < 0.0001$). With ongoing training, however, mice again developed a spatial preference for the new platform position ($F_{3,66} = 18.9$, $P < 0.0001$; Fig. 5B) to a same extent in both genotypes (*genotype*: $F_{1,22} = 0.724$, $P = 0.404$; *genotype* × *day*: $F_{3,66} = 0.220$, $P = 0.882$).

We used another batch of mice to perform the classical Morris water maze under low light conditions (Fig. 5D–F). Confirming the results from the 2P water maze, mice from either genotype readily learned to locate the hidden platform (*genotype*: $F_{1,17} = 0.492$, $P = 0.493$; *day*: $F_{2,34} = 30.0$, $P < 0.0001$; genotype × day: $F_{2,34} = 0.653$, $P = 0.527$; Fig. 5D). In the subsequent probe trial, both genotypes selectively searched in the former target quadrant (*genotype*: $F_{1,17} = 1.13$, $P = 0.303$; *quadrant*: $F_{3,51} = 62.9$, $P < 0.0001$; *genotype* × *quadrant*: $F_{3,51} = 0.716$, $P = 0.547$; target >; Q1, Q2, Q4, $P < 0.001$; Fig. 5E–G).

Increased step-down avoidance in CNGA3$^{-/-}$ mice

In the step-down avoidance test, CNGA3$^{-/-}$ mice showed an increase in the latency 24 h after learning, compared with WT controls, which approached statistical significance ($t_{16} = 2.1$, $P = 0.052$; Fig. 5H). However, if we compared the development of step-down latencies from the training day (KO: 21.3 ± 6.1 seconds; WT: 10.3 ± 2.0 seconds) to the test day, a two-way ANOVA showed significant main effects of *genotype* ($F_{1,16} = 5.01$, $P = 0.040$) and *day* ($F_{1,16} = 59.8$, $P < 0.0001$), but no significant *genotype* × *day* interaction ($F_{1,16} = 3.56$, $P = 0.077$), indicating that CNGA3$^{-/-}$ mice might be generally slower in stepping down from the platform.

Intact contextual and sensitized fear but impaired auditory-cued fear memory in CNGA3$^{-/-}$ mice

To further characterize the role of CNGA3 in hippocampus- and amygdala-dependent behavior, we performed fear conditioning experiments with litter-matched CNGA3$^{+/+}$ and CNGA3$^{-/-}$ mice. Contextual fear memory depends both on the amygdala and the hippocampus (Anagnostaras *et al*. 1999), whereas the formation of auditory-cued fear memory is primarily amygdala dependent (LeDoux 2000). We tested the ability of WT and CNGA3$^{-/-}$ mice to associate either the context or the auditory stimulus (tone) with an aversive stimulus (electric shock). Mice of both genotypes froze significantly more in the conditioning context than in a neutral environment without tone presentation (*context*: $F_{1,22} = 62.03$, $P < 0.0001$). In agreement with the finding that CNGA3 null mutants performed normally in the hippocampus-dependent water maze test, we failed to observe significant differences in contextual fear conditioning between the two genotypes (*genotype*: $F_{1,22} = 0.03$, $P = 0.857$; *genotype* × *context*: $F_{1,22} = 0.07$, $P = 0.798$; Fig. 6A). Assessment of auditory-cued fear in the neutral environment showed that CNGA3$^{+/+}$ and CNGA3$^{-/-}$ mice showed increased freezing during the 3-min phase when the tone was presented compared to preceding 3 min without presentation of the tone (*tone*: $P < 0.0001$). However, freezing to the tone was significantly

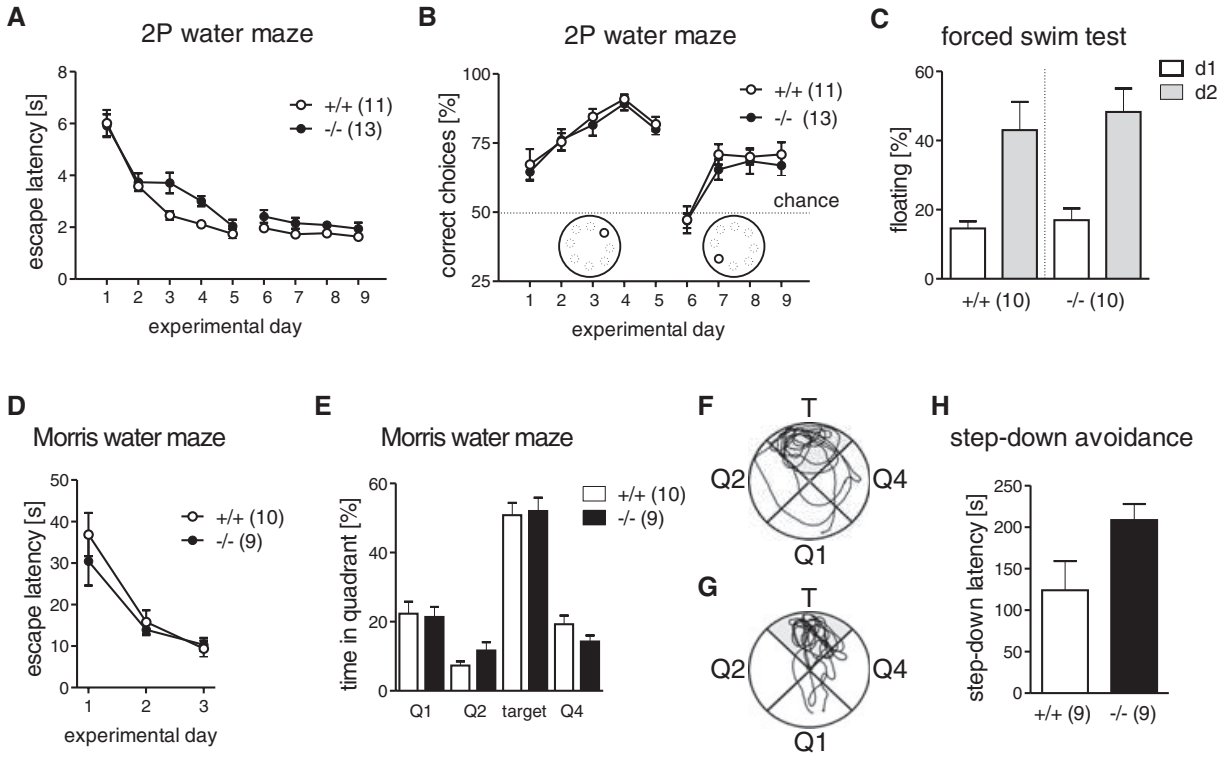

Figure 5: Spatial learning and inhibitory avoidance in CNGA3$^{-/-}$ mice. (A and B) Two platform discriminatory water maze (2P water maze). (A) Escape latencies and (B) the number of correct choices in a discriminatory water maze task of CNGA3$^{-/-}$ mice and CNGA3$^{+/+}$ littermate controls. Animals had to discriminate between two visible platforms, one remained in a fixed position from days 1 to 5 and days 6 to 9 (correct platform), and the other changed its position between two consecutive trials (incorrect platform). Data were merged per training session (10 trials) and animal (A) or normalized to the total number of choices (B). The position of the correct platform (bold) was changed between days 5 and 6, as indicated by the insets in (B). (C) Forced swimming test. Animals were forced to swim for 6 min on two consecutive days (d1, d2), and the time the mice spent floating was measured and normalized to the observation period. (D–G) Morris water maze – hidden platform task. (D) Escape latencies of CNGA3$^{-/-}$ mice and CNGA3$^{+/+}$ littermate controls. Animals had to locate a hidden platform on days 1–3. Data were merged per training session (six trials) and animal. (E) Probe trial. The hidden platform was removed on day 4 to assess reference memory during a 1-min probe trial. (F and G) Representative swim path of a CNGA3$^{+/+}$ mouse (F) and a littermate CNGA3$^{-/-}$ mouse (G) during the probe trial. Q, quadrant; T, target quadrant. (H) Step-down avoidance. Step-down latencies of CNGA3$^{-/-}$ mice and CNGA3$^{+/+}$ littermates 24 h after training. Data are presented as mean ± SEM, the number of animals in brackets.

reduced in CNGA3$^{-/-}$ mice compared with WT littermate controls (*genotype*: $F_{1,22} = 11.7$, $P = 0.002$; *genotype* × *tone*: $F_{1,22} = 12.2$, $P = 0.002$; Fig. 6B). The time–course of the freezing response analyzed in 60-second intervals further showed that these genotype differences were evident right from the onset of the tone and not because of differences in the grade of extinction of the freezing response during acute tone presentation (*genotype*: $F_{1,22} = 12.4$, $P = 0.002$; *time*: $F_{2,44} = 19.3$, $P < 0.0001$; *genotype* × *time*: $F_{2,44} = 0.9$, $P = 0.438$; Fig. 6C).

It is feasible that the impairment of auditory-cued fear memory observed in CNGA3$^{-/-}$ mice results from more general defects such as altered processing of the auditory stimulus/foot shock or changes of the emotional state. Therefore, we additionally performed a sensitization test in which the foot shock was presented without the tone on the conditioning day (Kamprath & Wotjak 2004), followed by exposure to the neutral tone 24 h later. In addition, we tested the ASRs of the KO mice. Wild-type and KO mice showed similar sensitized fear to the neutral tone (*genotype*: $F_{1,18} = 0.428$, $P = 0.521$; *tone*: $F_{1,18} = 26.7$, $P < 0.0001$; *genotype* × *tone*: $F_{1,18} = 2.71$, $P = 0.117$; Fig. 6D). Also foreground contextual fear (as assessed upon re-exposure to the conditioning context) showed the same intensity and specificity (as assessed by comparing freezing in the conditioning context and freezing before tone presentation in the test context) in the two genotypes (*genotype*: $F_{1,18} = 2.00$, $P = 0.173$; *context*: $F_{1,18} = 57.0$, $P < 0.0001$; *genotype* × *context*: $F_{1,18} = 0.32$, $P = 0.581$).

Although the similarities in sensitized fear speak against genotype differences in tone and shock perception, we additionally measured in other animals' ASRs to stimuli of increasing intensity and their modulation by PPs. We failed

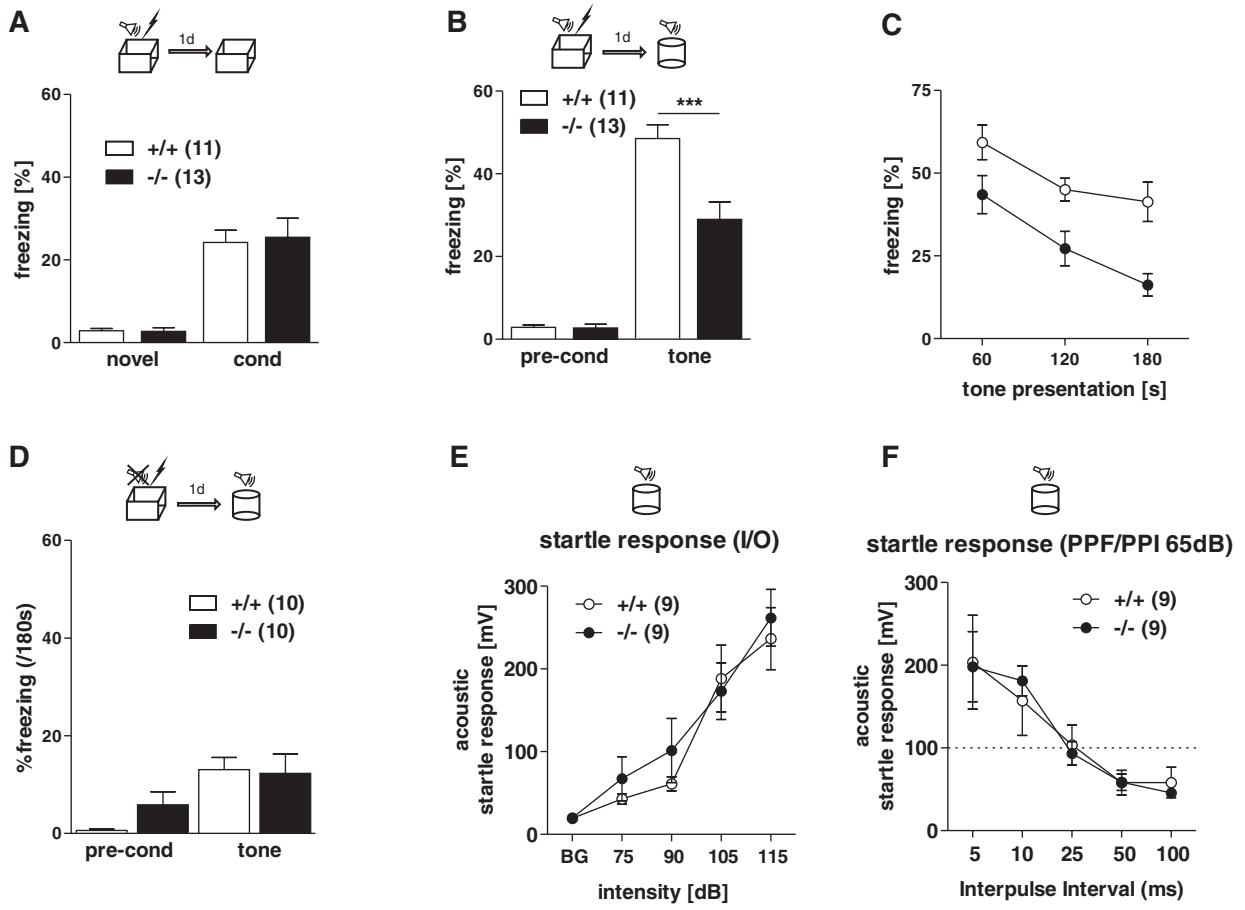

Figure 6: Intact contextual but impaired auditory-cued fear memory in CNGA3$^{-/-}$ mice. (A) Both CNGA3$^{-/-}$ and CNGA3$^{+/+}$ mice were re-exposed to the conditioning context and to the auditory stimulus in a neutral context at the day following auditory-cued fear conditioning. CNGA3$^{-/-}$ and CNGA3$^{+/+}$ mice showed the same freezing response to the conditioning context without tone presentation (background contextual memory). (B) CNGA3$^{-/-}$ mice froze significantly less to the tone in a neutral context than wild-type littermate controls (auditory-cued memory). (C) Analysis of the freezing response to the tone in 1-min bins showed that the differences in auditory-cued memory between CNGA3$^{+/+}$ (○) and CNGA3$^{-/-}$ (•) mice were persistent over the course of the 3-min tone presentation. (D) CNGA3$^{+/+}$ and CNGA3$^{-/-}$ mice showed a similar freezing response to the conditioning context and a 3-min tone the day after a single, unsignaled shock (sensitization). (E and F) Naïve CNGA3$^{+/+}$ and CNGA3$^{-/-}$ mice showed similar acoustic startle responses. (E) Input-output relation of the startle responses. (F) Prepulse facilitation (PPF) or PPI of the startle response to a 65-dB prepulse presented at different interpulse interval. Data are presented as mean ± SEM; BG, background noise.

to observe differences in ASR (*genotype*: $F_{1,16} = 0.303$, $P = 0.590$; *intensity:* $F_{4,64} = 36.2$, $P < 0.0001$; *genotype* × *intensity:* $F_{4,64} = 0.488$, $P = 0.744$; Fig. 6E). In addition, mice showed the same PP facilitation and PPI with a PP intensity of 65 dB and interpulse intervals smaller or greater than 25 milliseconds (*genotype*: $F_{1,16} = 0.0$, $P = 0.983$; *interpulse interval:* $F_{4,64} = 23.6$, $P < 0.0001$; *genotype* × *interpulse interval:* $F_{4,64} = 0.287$, $P = 0.885$; Fig. 6F). Results with PP intensities of 55 and 75 dB showed essentially the same findings and are omitted for the sake of clarity and brevity.

Together, these findings support a modulatory role of CNGA3 channels for the formation of the tone-shock association in the amygdala.

Discussion

It has been shown that nitric oxide (NO)/cGMP signaling can support synaptic plasticity and consolidation of memory via stimulation of the cGMP-dependent protein kinase I (cGKI) (Feil & Kleppisch 2008; Kleppisch *et al*. 2003; Ota *et al*. 2008; Paul *et al*. 2008). In the present study, we report expression of the cone-type CNGA3 channel in mouse amygdala and hippocampus. Although the level of expression was found to be very low, the observed localization of CNGA3 in neuronal fibers suggests a role of this ion channel in synaptic function. Cyclic nucleotide-gated channels represent alternative targets for regulation by cGMP and may, thus, also contribute to the regulation of fear memory formation and related synaptic

plasticity. Heteromeric CNG channels containing the CNGA3 subunit are ideally suited to control these functions as they are activated by low micromolar concentrations of cGMP, do not inactivate and are highly permeable for calcium ions (Biel *et al*. 1994; Frings *et al*. 1995). Here, we show that CNGA3-containing channels are critically involved in the regulation of synaptic plasticity in the hippocampus. It is well established that LTP in the CA1 region of the hippocampus is triggered by postsynaptic Ca^{2+} entry mediated principally by *N*-methyl-D-aspartate (NMDA) receptors (Lynch 2004; Malenka & Nicoll 1999). One could, therefore, assume that CNGA3 channels expressed postsynaptically in hippocampal pyramidal cells might support the induction of LTP. Contrary to this expectation, mice lacking the CNGA3 channel showed enhanced LTP following strong tetanic stimulation, implying that one of the biological functions of the CNGA3 channel in hippocampal neurons is to constrain LTP from a maximum. A possible explanation could be that distinct Ca^{2+} sources in a neuron may by tuned to a specific signaling pathway with different, even opposite, effects on the induction and maintenance of LTP (Futatsugi *et al*. 1999; Nagase *et al*. 2003). Alternatively, the functional effect of a channel protein might be determined by its selective localization to pre- or postsynaptic structures. For example, CNGA3 channels may affect transmitter release by controlling the membrane potential of presynaptic terminals. In line with this view, Murphy and Isaacson (2003) reported that transmission at synapses between olfactory sensory neurons and olfactory bulb neurons is controlled by a CNG channel. Strongly activated, CNG channel-mediated currents may cause marked depolarization of presynaptic fibers resulting in inactivation of voltage-dependent Na^{+} channels and, thus, suppression of action potential propagation into nerve terminals of olfactory sensory neurons. It may be possible that CNGA3 serves a similar inhibitory role in afferent fibers of Schaffer collateral synapses. In support of this hypothesis, we observed localization of the CNGA3 protein in presynaptic fibers.

Synaptic plasticity is thought to provide a cellular substrate for learning and memory (Martin *et al*. 2000). Therefore, the question arises as to whether enhanced hippocampal LTP in CNGA3$^{-/-}$ mice is paralleled by superior learning and memory similar to mice overexpressing the NR2B subunit of the NMDA receptor (Tang *et al*. 1999). Owing to the loss of CNGA3 in the retina, CNGA3$^{-/-}$ mice have impaired daylight vision, but have normal rod photoreceptor-mediated vision (Biel *et al*. 1999). We, therefore, tested CNGA3$^{-/-}$ mice for their spatial learning in water maze tests at dim light conditions that favor rod photoreceptor-mediated vision. Under these conditions, CNGA3$^{-/-}$ mice showed intact spatial learning and memory that was indistinguishable from the performance of CNGA3$^{+/+}$ littermate controls in both water maze paradigms (2P water maze and hidden platform Morris water maze). The fact that animals of either genotype displayed a significant drop in their searching accuracy after reversal of the platform position at day 6 of the 2P water maze and developed the same preference for the target quadrant in the probe trial of the Morris water maze indicates that mice from both groups oriented themselves along distal landmarks for locating the correct platform. This allocentric navigation requires a structurally and functionally intact hippocampal formation (Arns *et al*. 1999; D'Hooge & De Deyn 2001; Lipp & Wolfer 1998). The difference in the escape latencies between CNGA3$^{-/-}$ and CNGA3$^{+/+}$ mice at days 3 and 4 of the 2P water maze seems to be of minor biological significance, in particular, as the latencies do not affect the spatial preference scores and reach similar asymptotic levels toward the end of the 2P water maze test. Moreover, the difference in escape latencies does not reflect enhanced stress susceptibility in CNGA3$^{-/-}$ mice, as their performance in the forced swimming task was comparable to CNGA3$^{+/+}$ mice.

We additionally tested the CNGA3$^{-/-}$ mice for contextual fear memory, a task that also critically depends on an intact hippocampal formation (Anagnostaras *et al*. 1999; Gerlai 1998; Kim & Fanselow 1992), but not exclusively depends on vision. There was no significant difference between CNGA3$^{-/-}$ and CNGA3$^{+/+}$ mice in contextual fear memory, neither following the background (conditioning) nor the foreground protocol (sensitization). These data further support our previous conclusion of normal hippocampus-dependent learning in CNGA3$^{-/-}$ mice.

There is an increasing number of studies documenting a dissociation between alterations in CA1 LTP and spatial navigation, e.g. in the water maze. Specifically, enhanced LTP can correlate with improved or normal and even impaired spatial learning (Dean *et al*. 2009; Futatsugi *et al*. 1999; Hoeffer *et al*. 2008; Jun *et al*. 1998; Kaksonen *et al*. 2002; Kim *et al*. 2009; Migaud *et al*. 1998; Rutten *et al*. 2008; Tang *et al*. 1999). Furthermore, Reisel *et al*. (2002) showed that impaired CA1 LTP might be associated with deficits in spatial working memory rather than spatial reference memory. Therefore, we cannot exclude the possibility that moderate changes in hippocampus-dependent learning of CNGA3$^{-/-}$ mice remained undetected by our learning paradigms (associated with fear, stress and/or high physical demand). We therefore tested the KO mice in the more simple, less demanding step-down avoidance test. Interestingly, CNGA3$^{-/-}$ mice showed longer step-down latencies compared with CNGA3$^{+/+}$ mice, which may reflect superior hippocampus-dependent learning (Murgatroyd *et al*. 2009). However, we cannot preclude that CNGA3$^{-/-}$ mice are generally inhibited in stepping down from the platform as indicated by the lack of a significant *day* × *genotype* interaction. Future studies will have to address potential genotype differences in locomotor activity or innate anxiety in more detail.

To evaluate the role of CNGA3 for behavior related to the amygdala, we examined the performance of CNGA3$^{-/-}$ mice and their WT littermates in Pavlovian fear conditioning (Rodrigues *et al*. 2004). In contrast to the preserved contextual fear memory, CNGA3$^{-/-}$ mice showed a specific deficit in amygdala-dependent learning, as they froze less to the tone in a neutral environment at the day following conditioning, compared with CNGA3$^{+/+}$ control mice. The time–course of the freezing response implies that the reduced fear memory does not result from differences in acute adaptation to the tone over the course of the 3-min presentation. Moreover, it seems to be related specifically to deficits in the tone-shock association rather than to *a priori* differences between the WT and CNGA3 null mutants in

pain perception or basic processing of auditory signals. Each of those factors would be expected to affect the reaction to the tone following sensitization as well (Kamprath & Wotjak 2004). Contrary to this assumption, the corresponding responses were similar in CNGA3$^{-/-}$ and CNGA3$^{+/+}$ mice. In agreement with normal acute pain perception, CNGA3$^{-/-}$ mice showed intact immediate responses to acute noxious thermal and mechanical stimulation (unpublished data). The lack of genotype differences in processing of acoustic stimuli could be confirmed by measuring ASRs.

A selective impairment in the auditory-cued component but no alterations in the contextual component of fear conditioning were also observed in mice lacking the muscarinic acetylcholine receptor M1 (Miyakawa *et al*. 2001), but also in cGKI-deficient mice (Paul *et al*. 2008). The latter implies the presence of distinct cGMP-dependent pathways that support the formation of fear memory in the amygdala. The lack of impairment in contextual fear memory in CNGA3$^{-/-}$ mice may also result from differential effects of CNGA3 at hippocampal and amygdala level (e.g. improved hippocampal function may counterbalance decreased amygdala function to produce a normal contextual fear response). The deficit in auditory-cued fear memory in cGKI-deficient mice is accompanied by a marked reduction of LTP in the LA (Paul *et al*. 2008). As we did not observe any significant effect of the deletion of CNGA3 on synaptic plasticity in the LA or the BLA, the exact mechanism of how CNGA3 modulates the tone-shock association is still unclear.

In conclusion, our study adds a new entry to the list of physiological functions of the CNGA3 channel. While this channel was so far considered to be specifically important for cone-mediated vision and odor detection in a subset of olfactory neurons, we show here that CNGA3 is also involved in the modulation of hippocampal plasticity and the amygdala-dependent consolidation of fear memory. Mutations in CNGA3 account for more than 20% of all cases with autosomal recessive achromatopsia (Kohl *et al*. 2005; Michaelides *et al*. 2004). It would be interesting to test whether achromat patients with loss-of-function mutations in CNGA3 also show alterations in formation of aversive memories.

References

Anagnostaras, S.G., Maren, S. & Fanselow, M.S. (1999) Temporally graded retrograde amnesia of contextual fear after hippocampal damage in rats: within-subjects examination. *J Neurosci* **19**, 1106–1114.

Arns, M., Sauvage, M. & Steckler, T. (1999) Excitotoxic hippocampal lesions disrupt allocentric spatial learning in mice: effects of strain and task demands. *Behav Brain Res* **106**, 151–164.

Biel, M. & Michalakis, S. (2007) Function and dysfunction of CNG channels: insights from channelopathies and mouse models. *Mol Neurobiol* **35,** 266–277.

Biel, M. & Michalakis, S. (2009) Cyclic nucleotide-gated channels. *Handb Exp Pharmacol* **191**, 111–136.

Biel, M., Zong, X., Distler, M., Bosse, E., Klugbauer, N., Murakami, M., Flockerzi, V. & Hofmann, F. (1994) Another member of the cyclic nucleotide-gated channel family, expressed in testis, kidney, and heart. *Proc Natl Acad Sci U S A* **91**, 3505–3509.

Biel, M., Seeliger, M., Pfeifer, A., Kohler, K., Gerstner, A., Ludwig, A., Jaissle, G., Fauser, S., Zrenner, E. & Hofmann, F. (1999) Selective loss of cone function in mice lacking the cyclic nucleotide-gated channel CNG3. *Proc Natl Acad Sci U S A* **96**, 7553–7557.

Craven, K.B. & Zagotta, W.N. (2006) CNG and HCN channels: two peas, one pod. *Annu Rev Physiol* **68**, 375–401.

Dean, C., Liu, H., Dunning, F.M., Chang, P.Y., Jackson, M.B. & Chapman, E.R. (2009) Synaptotagmin-IV modulates synaptic function and long-term potentiation by regulating BDNF release. *Nat Neurosci* **12**, 767–776.

D'Hooge, R. & De Deyn, P.P. (2001) Applications of the Morris water maze in the study of learning and memory. *Brain Res Brain Res Rev* **36**, 60–90.

Feil, R. & Kleppisch, T. (2008) NO/cGMP-dependent modulation of synaptic transmission. *Handb Exp Pharmacol* **184**, 529–560.

Frings, S., Seifert, R., Godde, M. & Kaupp, U.B. (1995) Profoundly different calcium permeation and blockage determine the specific function of distinct cyclic nucleotide-gated channels. *Neuron* **15**, 169–179.

Futatsugi, A., Kato, K., Ogura, H., Li, S.T., Nagata, E., Kuwajima, G., Tanaka, K., Itohara, S. & Mikoshiba, K. (1999) Facilitation of NMDAR-independent LTP and spatial learning in mutant mice lacking ryanodine receptor type 3. *Neuron* **24**, 701–713.

Gerlai, R. (1998) Contextual learning and cue association in fear conditioning in mice: a strain comparison and a lesion study. *Behav Brain Res* **95**, 191–203.

Hoeffer, C.A., Tang, W., Wong, H., Santillan, A., Patterson, R.J., Martinez, L.A., Tejada-Simon, M.V., Paylor, R., Hamilton, S.L. & Klann, E. (2008) Removal of FKBP12 enhances mTOR-Raptor interactions, LTP, memory, and perseverative/repetitive behavior. *Neuron* **60**, 832–845.

Jun, K., Choi, G., Yang, S.G., Choi, K.Y., Kim, H., Chan, G.C., Storm, D.R., Albert, C., Mayr, G.W., Lee, C.J. & Shin, H.S. (1998) Enhanced hippocampal CA1 LTP but normal spatial learning in inositol 1,4,5-trisphosphate 3-kinase(A)-deficient mice. *Learn Mem* **5**, 317–330.

Kaksonen, M., Pavlov, I., Voikar, V., Lauri, S.E., Hienola, A., Riekki, R., Lakso, M., Taira, T. & Rauvala, H. (2002) Syndecan-3-deficient mice exhibit enhanced LTP and impaired hippocampus-dependent memory. *Mol Cell Neurosci* **21**, 158–172.

Kamprath, K. & Wotjak, C.T. (2004) Nonassociative learning processes determine expression and extinction of conditioned fear in mice. *Learn Mem* **11**, 770–786.

Kaupp, U.B. & Seifert, R. (2002) Cyclic nucleotide-gated ion channels. *Physiol Rev* **82**, 769–824.

Kemp, N. & Bashir, Z.I. (1997) NMDA receptor-dependent and - independent long-term depression in the CA1 region of the adult rat hippocampus *in vitro*. *Neuropharmacology* **36**, 397–399.

Kim, J.J. & Fanselow, M.S. (1992) Modality-specific retrograde amnesia of fear. *Science* **256**, 675–677.

Kim, M.H., Choi, J., Yang, J., Chung, W., Kim, J.H., Paik, S.K., Kim, K., Han, S., Won, H., Bae, Y.S., Cho, S.H., Seo, J., Bae, Y.C., Choi, S.Y. & Kim, E. (2009) Enhanced NMDA receptor-mediated synaptic transmission, enhanced long-term potentiation, and impaired learning and memory in mice lacking IRSp53. *J Neurosci* **29**, 1586–1595.

Kleppisch, T., Pfeifer, A., Klatt, P., Ruth, P., Montkowski, A., Fassler, R. & Hofmann, F. (1999) Long-term potentiation in the hippocampal CA1 region of mice lacking cGMP-dependent kinases is normal and susceptible to inhibition of nitric oxide synthase. *J Neurosci* **19**, 48–55.

Kleppisch, T., Wolfsgruber, W., Feil, S., Allmann, R., Wotjak, C.T., Goebbels, S., Nave, K.A., Hofmann, F. & Feil, R. (2003) Hippocampal cGMP-dependent protein kinase I supports an age- and protein synthesis-dependent component of long-term potentiation but is not essential for spatial reference and contextual memory. *J Neurosci* **23**, 6005–6012.

Kohl, S., Marx, T., Giddings, I., Jagle, H., Jacobson, S.G., Apfelstedt-Sylla, E., Zrenner, E., Sharpe, L.T. & Wissinger, B. (1998) Total colour blindness is caused by mutations in the gene encoding the alpha-subunit of the cone photoreceptor cGMP-gated cation channel. *Nat Genet* **19**, 257–259.

Kohl, S., Varsanyi, B., Antunes, G.A. *et al*. (2005) CNGB3 mutations account for 50% of all cases with autosomal recessive achromatopsia. *Eur J Hum Genet* **13**, 302–308.
Kuzmiski, J.B. & MacVicar, B.A. (2001) Cyclic nucleotide-gated channels contribute to the cholinergic plateau potential in hippocampal CA1 pyramidal neurons. *J Neurosci* **21**, 8707–8714.
LeDoux, J.E. (2000) Emotion circuits in the brain. *Annu Rev Neurosci* **23**, 155–184.
Leinders-Zufall, T., Cockerham, R.E., Michalakis, S., Biel, M., Garbers, D.L., Reed, R.R., Zufall, F. & Munger, S.D. (2007) Contribution of the receptor guanylyl cyclase GC-D to chemosensory function in the olfactory epithelium. *Proc Natl Acad Sci U S A* **104**, 14507–14512.
Lipp, H.P. & Wolfer, D.P. (1998) Genetically modified mice and cognition. *Curr Opin Neurobiol* **8**, 272–280.
Lynch, M.A. (2004) Long-term potentiation and memory. *Physiol Rev* **84**, 87–136.
Malenka, R.C. & Nicoll, R.A. (1999) Long-term potentiation – a decade of progress? *Science* **285**, 1870–1874.
Marsicano, G., Wotjak, C.T., Azad, S.C., Bisogno, T., Rammes, G., Cascio, M.G., Hermann, H., Tang, J., Hofmann, C., Zieglgansberger, W., Di Marzo, V. & Lutz, B. (2002) The endogenous cannabinoid system controls extinction of aversive memories. *Nature* **418**, 530–534.
Martin, S.J., Grimwood, P.D. & Morris, R.G. (2000) Synaptic plasticity and memory: an evaluation of the hypothesis. *Annu Rev Neurosci* **23**, 649–711.
Michaelides, M., Hunt, D.M. & Moore, A.T. (2004) The cone dysfunction syndromes. *Br J Ophthalmol* **88**, 291–297.
Michalakis, S., Geiger, H., Haverkamp, S., Hofmann, F., Gerstner, A. & Biel, M. (2005) Impaired opsin targeting and cone photoreceptor migration in the retina of mice lacking the cyclic nucleotide-gated channel CNGA3. *Invest Ophthalmol Vis Sci* **46**, 1516–1524.
Migaud, M., Charlesworth, P., Dempster, M., Webster, L.C., Watabe, A.M., Makhinson, M., He, Y., Ramsay, M.F., Morris, R.G., Morrison, J.H., O'Dell, T.J. & Grant, S.G. (1998) Enhanced long-term potentiation and impaired learning in mice with mutant postsynaptic density-95 protein. *Nature* **396**, 433–439.
Miyakawa, T., Yamada, M., Duttaroy, A. & Wess, J. (2001) Hyperactivity and intact hippocampus-dependent learning in mice lacking the M1 muscarinic acetylcholine receptor. *J Neurosci* **21**, 5239–5250.
Moosmang, S., Haider, N., Klugbauer, N., Adelsberger, H., Langwieser, N., Muller, J., Stiess, M., Marais, E., Schulla, V., Lacinova, L., Goebbels, S., Nave, K.A., Storm, D.R., Hofmann, F. & Kleppisch, T. (2005) Role of hippocampal Cav1.2 Ca2+ channels in NMDA receptor-independent synaptic plasticity and spatial memory. *J Neurosci* **25**, 9883–9892.
Munger, S.D., Leinders-Zufall, T. & Zufall, F. (2009) Subsystem organization of the mammalian sense of smell. *Annu Rev Physiol* **71**, 115–140.
Murgatroyd, C., Patchev, A.V., Wu, Y., Micale, V., Bockmuhl, Y., Fischer, D., Holsboer, F., Wotjak, C.T., Almeida, O.F. & Spengler, D. (2009) Dynamic DNA methylation programs persistent adverse effects of early-life stress. *Nat Neurosci* **12**, 1559–1566.
Murphy, G.J. & Isaacson, J.S. (2003) Presynaptic cyclic nucleotide-gated ion channels modulate neurotransmission in the mammalian olfactory bulb. *Neuron* **37**, 639–647.
Nagase, T., Ito, K.I., Kato, K., Kaneko, K., Kohda, K., Matsumoto, M., Hoshino, A., Inoue, T., Fujii, S., Kato, H. & Mikoshiba, K. (2003) Long-term potentiation and long-term depression in hippocampal CA1 neurons of mice lacking the IP(3) type 1 receptor. *Neuroscience* **117**, 821–830.
Ota, K.T., Pierre, V.J., Ploski, J.E., Queen, K. & Schafe, G.E. (2008) The NO-cGMP-PKG signaling pathway regulates synaptic plasticity and fear memory consolidation in the lateral amygdala via activation of ERK/MAP kinase. *Learn Mem* **15**, 792–805.
Parent, A., Schrader, K., Munger, S.D., Reed, R.R., Linden, D.J. & Ronnett, G.V. (1998) Synaptic transmission and hippocampal long-term potentiation in olfactory cyclic nucleotide-gated channel type 1 null mouse. *J Neurophysiol* **79**, 3295–3301.
Paul, C., Schoberl, F., Weinmeister, P., Micale, V., Wotjak, C.T., Hofmann, F. & Kleppisch, T. (2008) Signaling through cGMP-dependent protein kinase I in the amygdala is critical for auditory-cued fear memory and long-term potentiation. *J Neurosci* **28**, 14202–14212.
Rammes, G., Steckler, T., Kresse, A., Schutz, G., Zieglgansberger, W. & Lutz, B. (2000) Synaptic plasticity in the basolateral amygdala in transgenic mice expressing dominant-negative cAMP response element-binding protein (CREB) in forebrain. *Eur J Neurosci* **12**, 2534–2546.
Reisel, D., Bannerman, D.M., Schmitt, W.B., Deacon, R.M., Flint, J., Borchardt, T., Seeburg, P.H. & Rawlins, J.N. (2002) Spatial memory dissociations in mice lacking GluR1. *Nat Neurosci* **5**, 868–873.
Rodrigues, S.M., Schafe, G.E. & LeDoux, J.E. (2004) Molecular mechanisms underlying emotional learning and memory in the lateral amygdala. *Neuron* **44**, 75–91.
Rutten, K., Misner, D.L., Works, M., Blokland, A., Novak, T.J., Santarelli, L. & Wallace, T.L. (2008) Enhanced long-term potentiation and impaired learning in phosphodiesterase 4D-knockout (PDE4D) mice. *Eur J Neurosci* **28**, 625–632.
Tang, Y.P., Shimizu, E., Dube, G.R., Rampon, C., Kerchner, G.A., Zhuo, M., Liu, G. & Tsien, J.Z. (1999) Genetic enhancement of learning and memory in mice. *Nature* **401**, 63–69.

Acknowledgments

We thank Anja Mederer for help with behavioral experiments and Jennifer Schmidt for technical help. This work was supported by the Deutsche Forschungsgemeinschaft (KL1172/4-1 to T.K.).